Extension of the Collector Charge Description for Compact Bipolar Epilayer Models

Leo C. N. de Vreede, Henk C. de Graaff, Joseph L. Tauritz, *Member, IEEE*, and Roel G. F. Baets, *Senior Member, IEEE*

***Abstract*— In this paper, an extension to the collector charge description for compact bipolar epilayer models is presented. With this extension, monotonic f_T and Early-voltage behavior is ensured when transistor operation extends into the quasi-saturation region. The modification leads to a major improvement in the modeling of nonlinear distortion at high current levels and high frequencies.**

I. Introduction

During quasi-saturation (QS), when the internal base collector junction of a bipolar transistor becomes forward biased, the injection of minority charge carriers into the epilayer leads to the build up of a storage charge as well as to a substantial reduction of the epilayer resistance. This is described by Kull *et al.* [1], Jeong and Fossum [3], [4] and more completely by de Graaff and Kloosterman [7], [10] who included the influence of hot carriers and current spreading.

These improved epilayer models [1], [3], [7] are, however, particularly sensitive to their parameter values; slight deviations may produce erratic, nonmonotonic Early voltages and $f_T(I_c)$ behavior (see Figs. 8 and 10). The epilayer model used here is that of the Mextram model (see [10], [11]), with the following parameters.

V_{DC}	Built-in voltage of the base-collector junction.
I_{HC}	Critical current density for hot carriers.
R_{CV}	Ohmic epilayer resistance.
S_{CRCV}	Space-charge limited epilayer resistance.
S_{FH}	Factor for the epilayer current spreading.

When hot-carrier behavior ($I_{\mathrm{HC}} \rightarrow \infty$) is omitted, the Mextram epilayer description reduces to the Kull model [11]. In practice, epilayer parameter sets, especially V_{DC}, are extracted so as to avoid the nonmonotonic behavior, but this results in improper modeling of nonlinear distortion [9] at high current levels. This paper explores the underlying causes of these problems and proposes an improved formulation for the collector charge model. To this end, the Mextram model [5], [7] has been modified by adding an extra charge ΔQ_c, yielding a better modeling of signal distortion at high current levels and high frequencies and monotonicity in Early voltages and f_T fall-off characteristics. This modification can, in principle, also be applied to the models mentioned in [1], [3], and [4].

Manuscript received August 6, 1996; revised June 23, 1997. The review of this paper was arranged by Editor J. R. Hauser.

The authors are with the Delft Institute of Microelectronics and Submicron Technology, Microwave Component Group, Delft University of Technology, Delft, The Netherlands.

Publisher Item Identifier S 0018-9383(98)00287-1.

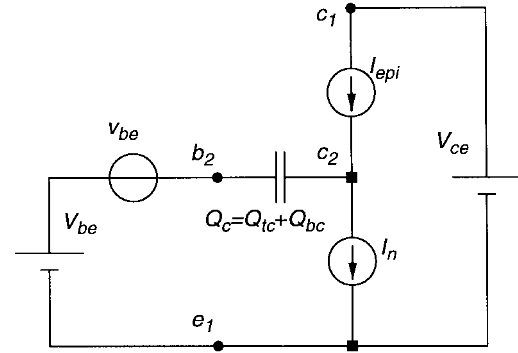

Fig. 1. Simplified circuit model of a bipolar transistor with a lightly-doped epilayer.

In order to make the problem more tractable and to help in finding a mathematical formulation for this extra charge ΔQ_c, we consider the ac signal transfer of a bipolar transistor with a lightly-doped epilayer.

II. Analysis of the Low-Frequency Small-Signal Transfer

At low frequencies and low driving conditions the distortion behavior of a device can be studied by investigating the derivatives of the ac transfer characteristics with respect to the base-emitter input voltage. This has been demonstrated in [9] and more extensively in [11]. The strongly simplified circuit of the bipolar epilayer transistor model used in this analysis is given in Fig. 1 (note that for these very low frequencies Q_c will have no effect and will be set to zero for this part of the analysis). The functions involved are now the main current $I_n(V_{b2e1}, V_{b2c2})$ and the epilayer current $I_{\mathrm{epi}}(V_{b2c2}, V_{b2c1})$ with the following small-signal definitions:

$$i_n = g_x v_{b2e1} + g_y v_{b2c2} \tag{1}$$

$$i_{\mathrm{epi}} = g_{\mathrm{epi}y} v_{b2c2} + g_{\mathrm{epi}z} v_{b2c1} \tag{2}$$

where

$$g_x = \left.\frac{\delta I_n}{\delta V_{b2e1}}\right|_{V_{b2c2}} \quad g_y = \left.\frac{\delta I_n}{\delta V_{b2c2}}\right|_{V_{b2e1}}$$

$$g_{\mathrm{epi}y} = \left.\frac{\delta I_{\mathrm{epi}}}{\delta V_{b2c2}}\right|_{V_{b2c1}} \quad g_{\mathrm{epi}z} = \left.\frac{\delta I_{\mathrm{epi}}}{\delta V_{b2c1}}\right|_{V_{b2c2}}. \tag{3}$$

AC short circuiting the output for the given network topology yields $v_{b2c1} = v_{b2e1}$ and of $i_n = i_{\mathrm{epi}}$. Using these conditions we can solve for the small-signal transconductance

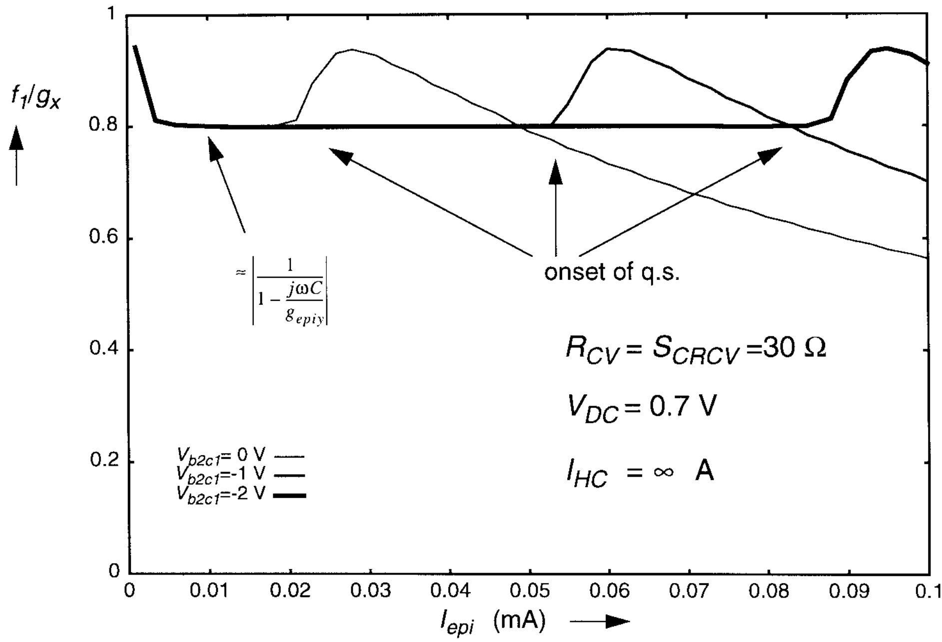

Fig. 2. Normalized transconductance (f_1/g_x) as function of the dc current using the Mextram epilayer model with $I_{\mathrm{HC}} \to \infty$ so that $S_{\mathrm{CRCV}} = R_{CV}$.

$i_{\mathrm{epi}}/v_{b2e1}$, leading to

$$\left.\frac{i_{\mathrm{epi}}}{v_{b2e1}}\right|_{V_{c1e1}} = g_x + g_y\left[\frac{g_{\mathrm{epi}z} - g_x}{g_y - g_{\mathrm{epi}y}}\right] = g_{\mathrm{epi}y}\left[\frac{g_{\mathrm{epi}z} - g_x}{g_y - g_{\mathrm{epi}y}}\right] + g_{\mathrm{epi}z}. \tag{4}$$

Plotting (4) as a function of the dc collector current (I_{epi}) yields information about the influence of the epilayer parameters on the distortion behavior, as has been demonstrated in [9] and [11].

III. Analysis of High-Frequency Small-Signal Transfer

At higher frequencies the base-collector depletion charge Q_{tc} becomes one of the dominant factors in the ac signal transfer when the transistor enters quasi-saturation (note that the total storage charge Q_{bc} will only have a significant value when the transistor is already in QS). The ac signal transfer is calculated using the circuit of Fig. 1. The functions involved are now $I_n(V_{b2e1}, V_{b2c2}), I_{\mathrm{epi}}(V_{b2c2}, V_{c1b2})$, and $Q_{tc}(V_{b2c2}, V_{b2c1})$. Concentrating on the small-signal transfer we use i_n, i_{epi} as defined in (1) and (2). The small-signal collector charge q_c is defined below

$$q_c = c_y v_{b2c2} + c_z v_{b2c1} \tag{5}$$

with

$$C_y = \left.\frac{\delta Q_{tc}}{\delta V_{b2c2}}\right|_{V_{b2c1}} \quad c_z = \left.\frac{\delta Q_{tc}}{\delta V_{b2c1}}\right|_{V_{b2c2}}. \tag{6}$$

The physical significance of c_y and c_z is considered in Appendix.

Due to the shorted output $(v_{b2c1} = v_{b2e1})$ we can solve again for the transconductance $(i_{\mathrm{epi}}/v_{b2e1})$, and find in place of (4)

$$\frac{i_{\mathrm{epi}}}{v_{b2e1}} = (j\omega c_z + g_{\mathrm{epi}z} - g_x)\left[\frac{g_{\mathrm{epi}y}}{g_y - (g_{\mathrm{epi}y} - j\omega c_y)}\right] + g_{\mathrm{epi}z} = f_1. \tag{7}$$

Plotting $i_{\mathrm{epi}}/v_{b2e1}$ as function of the dc collector current for sufficiently high values of ω_{cy} we find (given lower values of the built in base collector voltage V_{DC}) nonmonotonic behavior at the onset of quasi-saturation (QS) (see Fig. 2). This is caused by the current-dependent behavior of the multiplication term between square brackets in (7); rewriting

$$\left[\frac{g_{\mathrm{epi}y}}{g_y - (g_{\mathrm{epi}y} - j\omega c_y)}\right] = \frac{1}{\frac{g_y}{g_{\mathrm{epi}y}} - 1 + \frac{j\omega c_y}{g_{\mathrm{epi}y}}} = f_2. \tag{8}$$

In Fig. 3, f_2 is plotted as a function of the dc collector current $I_c(= I_{\mathrm{epi}})$. For reasons of simplicity Figs. 2 and 3 have been computed at 1 GHz with c_y constant (= 4 pF) and hot-carrier effects omitted. For low values of V_{DC} (e.g. 0.7 V), g_y will have a negligible value and there will be a sudden rise when QS sets in $(V_{b2c2} = V_{\mathrm{DC}})$. This can be suppressed by taking a higher value of V_{DC} (e.g. 0.8 V), see Fig. 3, but this will lead to incorrect modeling of distortion [9], [11]. The sudden rise in f_2 is due to the decrease in time constant when $c_y/g_{\mathrm{epi}y}$ falls to a low value, due to the reduction of the epilayer resistance in QS The same nonmonotonic behavior can be found in the $f_T(I_c)$ characteristics (e.g. see Fig. 10).

The drop in epilayer resistance is best illustrated by plotting $g_{\mathrm{epi}y}$ as a function of I_{epi} (see Fig. 4). It starts at a value of $1/R_{CV}$ and slowly decreases to (hot-carrier effects are now included) $1/S_{\mathrm{CRCV}}$ until at QS the $g_{\mathrm{epi}y}$ sharply rises. For a given $I_{\mathrm{epi}}, g_{\mathrm{epi}y}$ can be split into a nonsaturated part $g_{\mathrm{epi}ns}$ and a QS part Δg_{epi}. We define

$$g_{\mathrm{epi}ns} = \left|\frac{\delta I_{\mathrm{epi}ns}}{\delta V_{b2c2}}\right|_{V_{b2c1}} \quad \Delta g_{\mathrm{epi}} = \left.\frac{\delta \Delta I_{\mathrm{epi}}}{\delta V_{b2c2}}\right|_{V_{b2c1}} \tag{9}$$

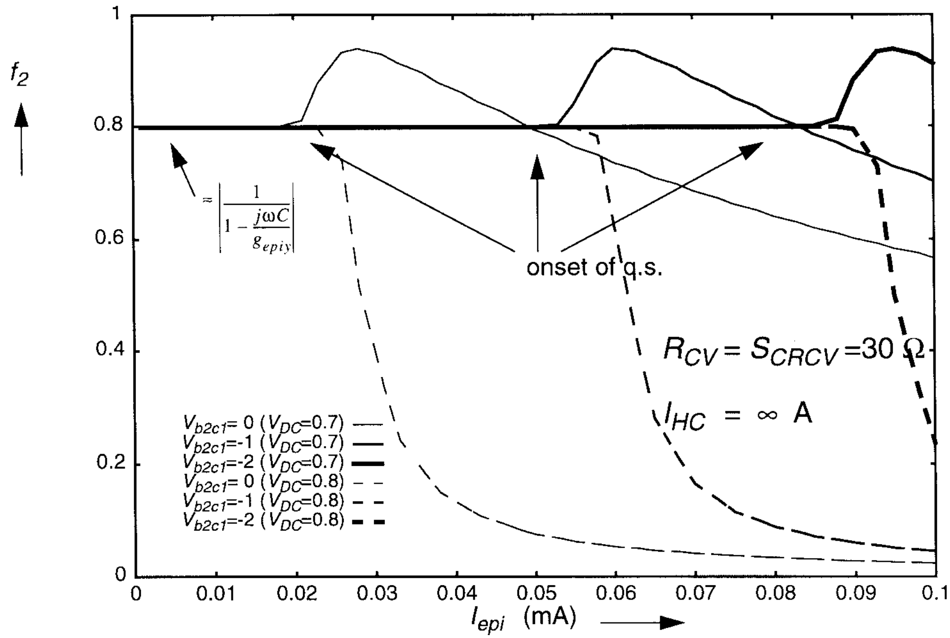

Fig. 3. Function (f_2) plotted as function of the dc current.

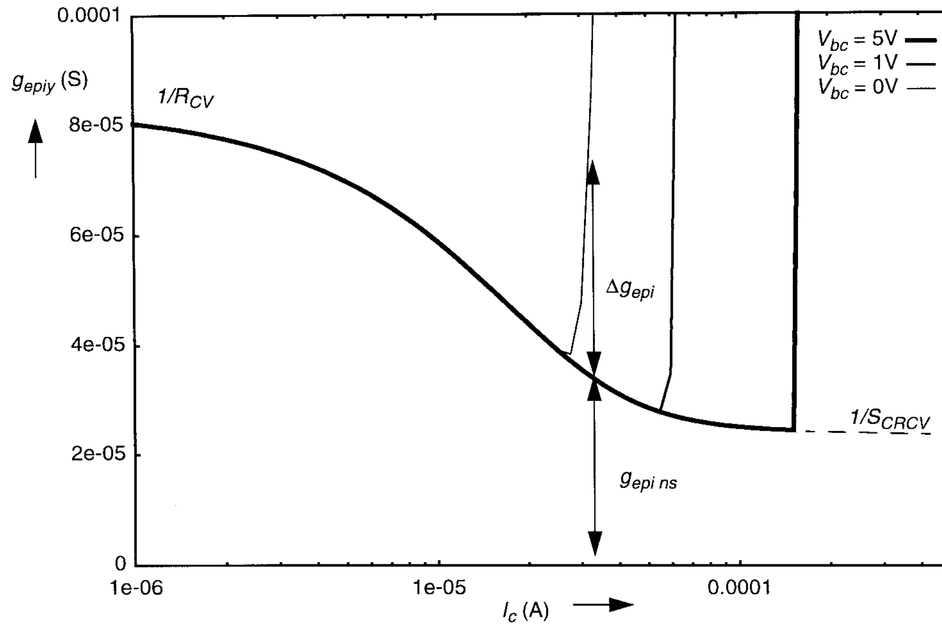

Fig. 4. The epilayer conductance $g_{\mathrm{epi}y}$ plotted as a function of the collector current, calculated with the modified Mextram model. V_{bc} is the external base-collector voltage $= V_{b2c1}+$ additional voltage drops.

with

$$\Delta I_{\mathrm{epi}} = I_{\mathrm{epi}} - I_{\mathrm{epi}ns}. \tag{10}$$

The equations for I_{epi} are given in [11], the nonsaturation current $I_{\mathrm{epi}ns}$ is given by

$$I_{\mathrm{epi}ns} = \frac{I_{\mathrm{HC}} S_{\mathrm{CRCV}} V_{c1c2} + V_{c1c2}^2}{S_{\mathrm{CRCV}}(I_{\mathrm{HC}} R_{\mathrm{CV}} + V_{c1c2})}. \tag{11}$$

Complete implementation of the Mextram model is described in [7]. To ensure monotonic behavior we add an extra capacitance Δc in such a way that the time constant

$$\frac{c_y}{g_{\mathrm{epi}y}} \Rightarrow \frac{c_y + \Delta c}{g_{\mathrm{epi}y}} = \frac{c_y + \Delta c}{g_{\mathrm{epi}ns} + \Delta g_{\mathrm{epi}}} = \frac{c_y}{g_{\mathrm{epi}ns}} \frac{\left(1 + \frac{\Delta c}{c_y}\right)}{\left(1 + \frac{\Delta g_{\mathrm{epi}}}{g_{\mathrm{epi}ns}}\right)} \tag{12}$$

behaves properly. This is the case if

$$\left(\frac{\Delta c}{c_y} = \frac{\Delta g_{\mathrm{epi}}}{g_{\mathrm{epi}ns}}\right) \Rightarrow \Delta c = \frac{\Delta g_{\mathrm{epi}}}{g_{\mathrm{epi}ns}} c_y. \tag{13}$$

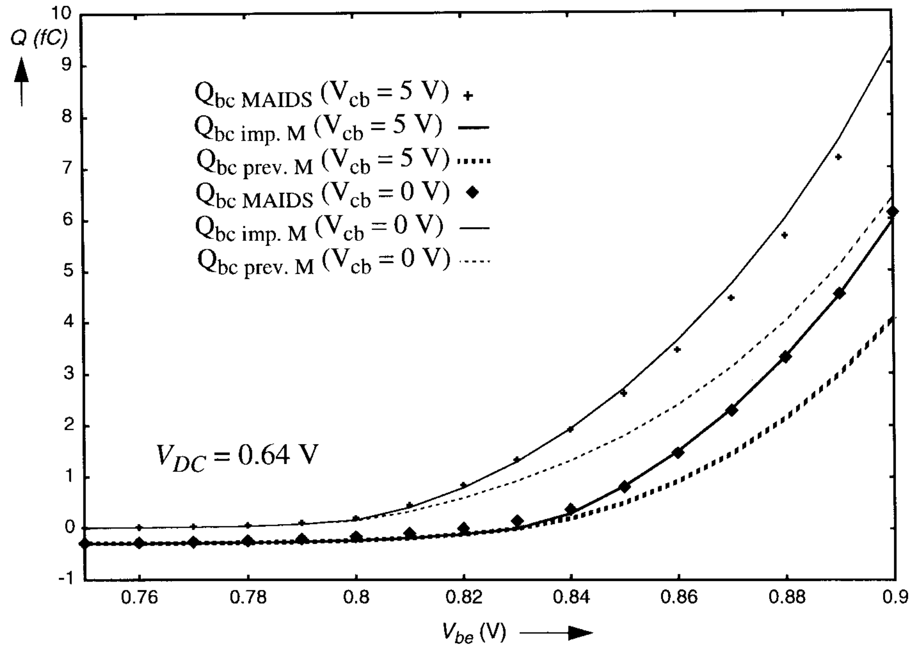

Fig. 5. The total base-collector charge using; MAIDS, the improved Mextram (with ΔQ_c) and the previous version of Mextram (without ΔQ_c).

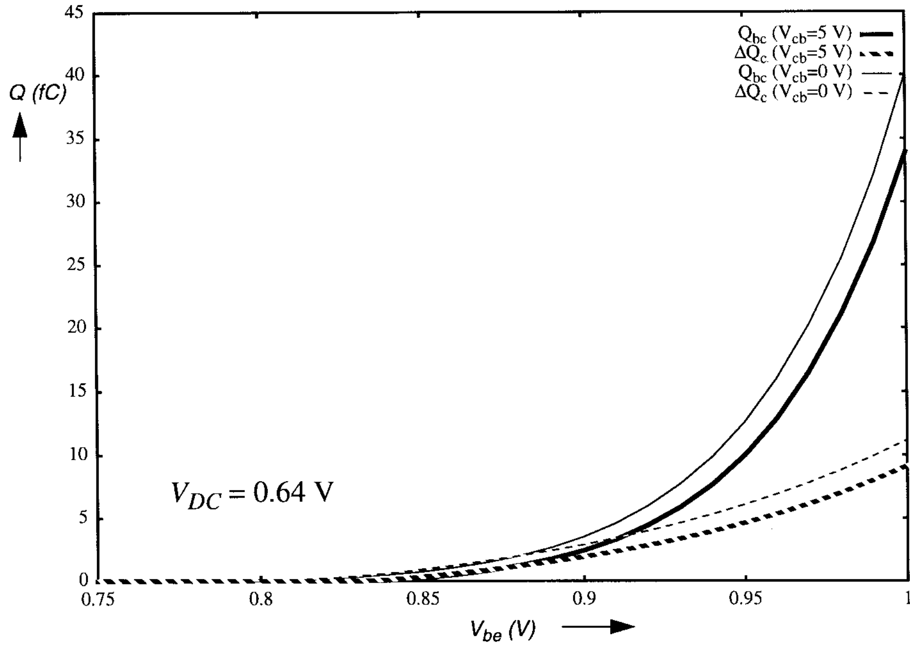

Fig. 6. The charge functions ΔQ_c and Q_{BC} obtained with the modified Mextram model.

The required extra charge ΔQ_c, ensuring monotonic Early voltages and $f_T(I_c)$ behavior is now given by

$$\Delta Q_c(V_{b2c2}, V_{b2c1}) = \int_0^{V_{b2c2}} c_y \left. \frac{\Delta g_{\text{epi}}}{g_{\text{epi}ns}} \right|_{V_{b2c2}} dV_{b2c2}. \quad (14)$$

Finally, in order to facilitate computability, the integral in (14) can be simplified into an analytical expression by noting that $c_y(V_{b2c2}, V_{b2c1})$ and $g_{\text{epi}ns}\ (V_{b2c2}, V_{b2c1})$ are slowly varying functions compared to $\Delta g_{\text{epi}}\ (V_{b2c2}, V_{b2c1})$, so

$$\Delta Q_c(V_{b2c2}, V_{b2c1}) \approx \frac{c_y}{g_{\text{epi}ns}} \int_0^{V_{b2c2}} \Delta g_{\text{epi}}\, dV_{b2c2} \quad (15)$$

which is equal to

$$\Delta Q_c(V_{b2c2}, V_{b2c1}) = \frac{c_y}{g_{\text{epi}ns}} [\Delta I_{\text{epi}}(V_{b2c2}, V_{b2c1}) - \Delta I_{\text{epi}}(0, V_{b2c1})]. \quad (16)$$

The maximum difference between the ΔQ_c's from (14) and (16) is about 10%. Note, that with the aid of (14) c.q. (16) the charge function ΔQ_c can be calculated based on the functional description of the base-collector depletion capacitance (c_y) and the epilayer current (I_{epi}). Using this formulation, ΔQ_c is *not* restricted to a specific epilayer model and can be calculated based on one of the models of [1], [3], [4], [7].

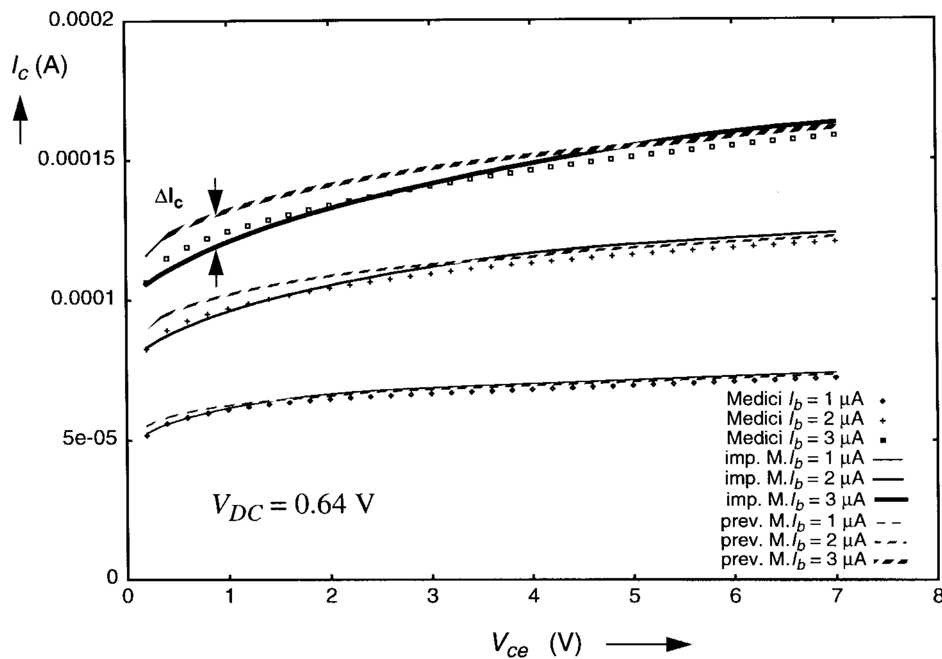

Fig. 7. $I_c(V_{ce})$ characteristic using the previous and improved Mextram model, compared to MEDICI.

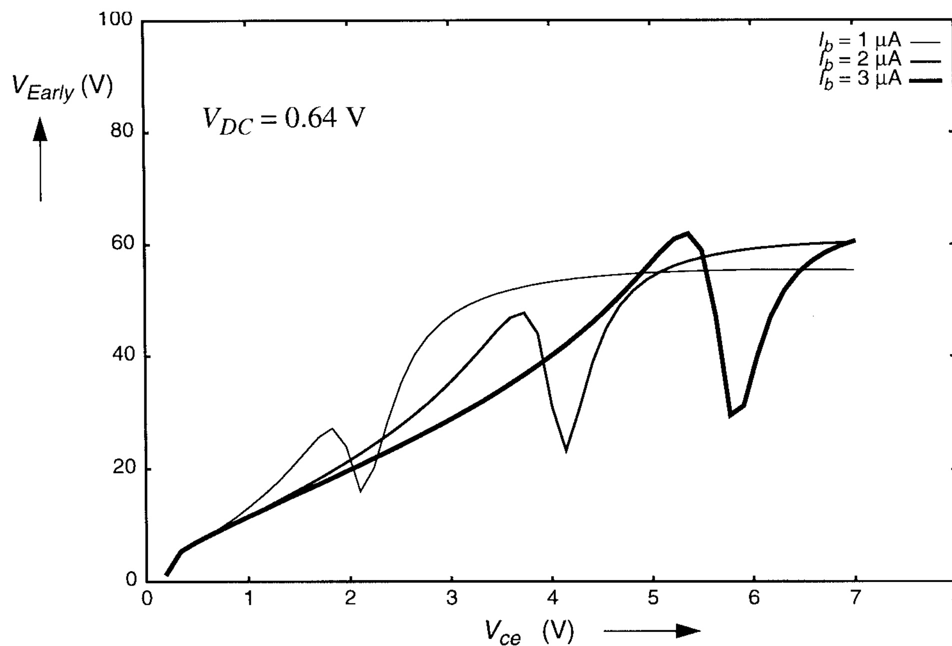

Fig. 8. Early-voltage characteristic using the previous Mextram model.

IV. The Physical Meaning of ΔQ_c

Physically speaking ΔQ_c represents mobile carrier charge stored in the space charge region surrounding the base-collector junction at high current levels. Verification of ΔQ_c by comparing the outcome of (14) or (16) with results obtained from device simulations can provide physical substantiation for the theory developed. The complication in such a comparison is that device simulations tend to lump together all the charge contributions. In order to calculate the base-collector charge using a device simulator one should therefore split the total charge into base-emitter and base-collector related components. Bias-, geometry-, and doping profile-dependent integration boundaries must be specified. This, combined with the fact that the charge components of interest are relatively small, led to the following strategy.

We simplify the boundary problem by using an one-dimensional (1-D) device structure and apply base charge partitioning to split the base-emitter and base-collector charges over the junctions [2]. The method used for the base charge partitioning has been proposed in [2] and is in conformance with the base doping profile and the current drive level. The function for the total base-collector charge (including the

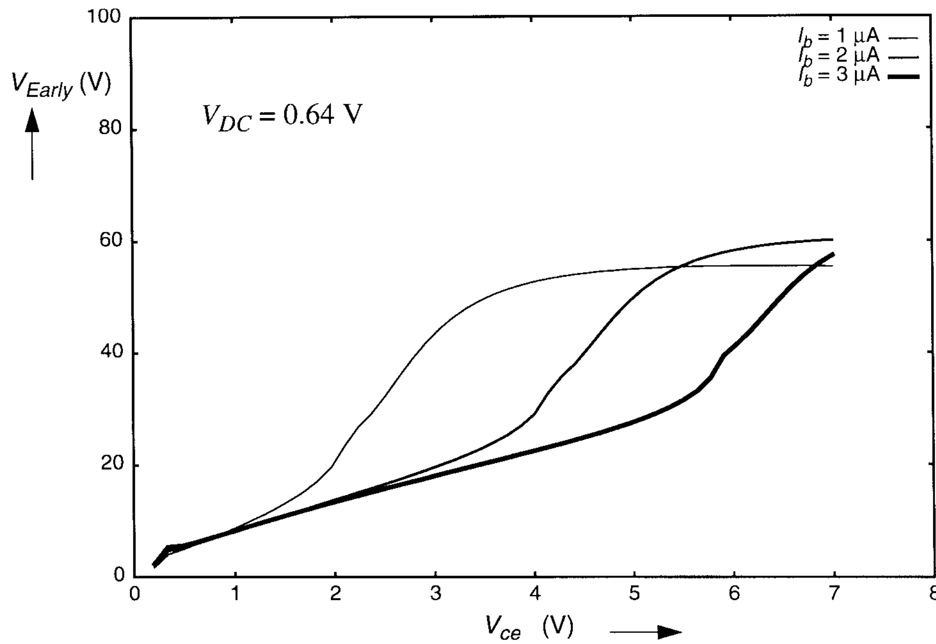

Fig. 9. Early-voltage characteristic using the improved Mextram model.

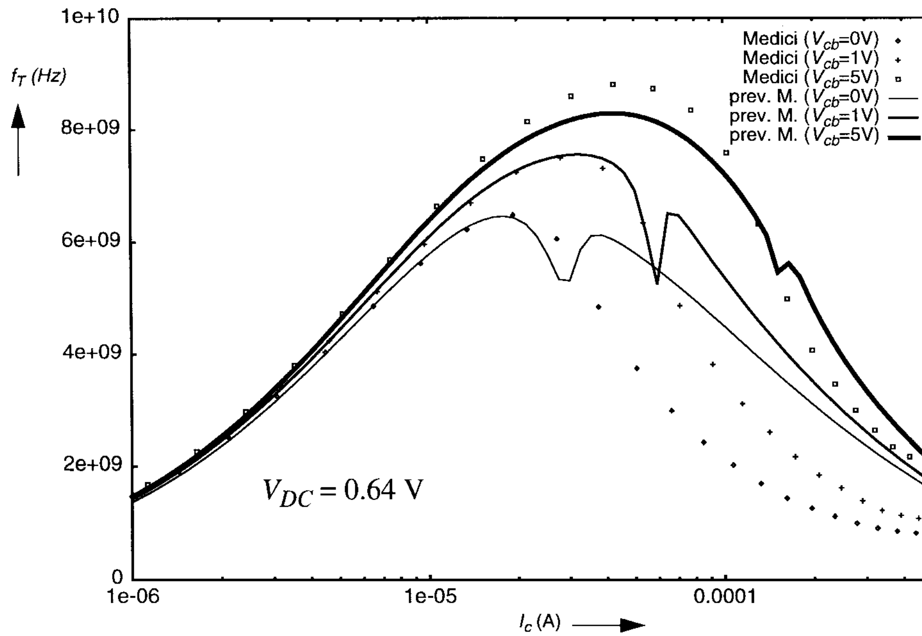

Fig. 10. $f_T(I_c)$ calculated using MEDICI for a device of 1 mm length and the previous version of Mextram.

epilayer charge storage) $Q_{bc\text{tot}}$ is then given by

$$Q_{bc\text{tot}} = \int_E^C qnA \cdot FC(\eta)\, d\eta \tag{17}$$

in which FC is a weighting function to split-off the base-collector charge. Using this method we are now able to compare the total charge storage in the collector with the charge components given by our compact model.

V. Results

Calculations based on the original as well as the modified Mextram model are compared with data obtained using the 1-D device simulator MAIDS [12] and the two-dimensional (2-D) device simulator MEDICI [6]. The transistor structure used in these simulations as described in [8], is based on SIMS measurements and is representative of present day bipolar transistor technology. The simulations with the Mextram model are performed using the Microwave Design System (MDS) of Hewlett Packard.

Physical support for the charge ΔQ_c can be found in Fig. 5. In this figure the total base-collector charge is plotted using the 1-D device simulator MAIDS, the modified Mextram model (with ΔQ_c), and the previous version of Mextram (without ΔQ_c). We note that the total charge calculated with

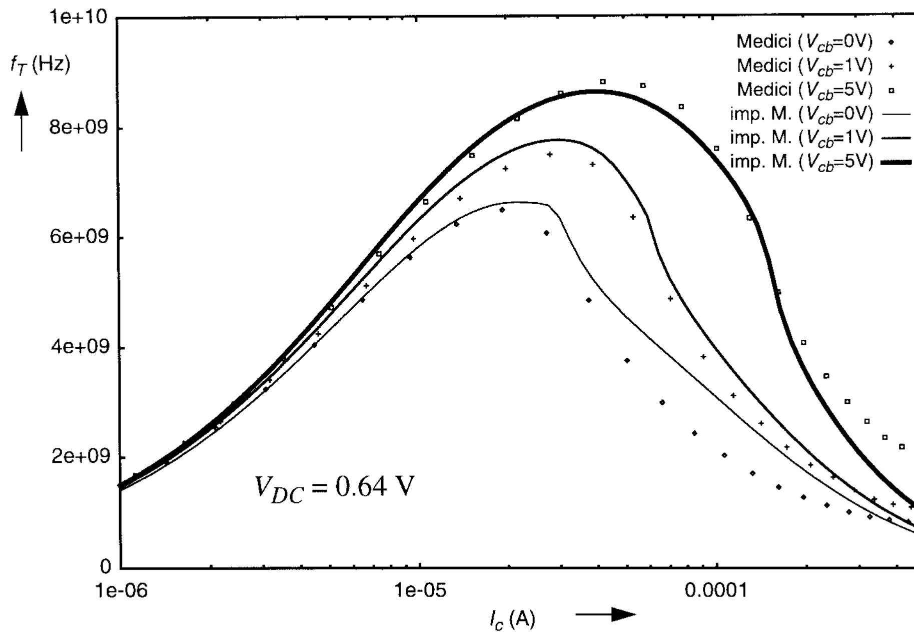

Fig. 11. The $f_T(I_c)$ characteristic calculated with MEDICI and the improved Mextram model.

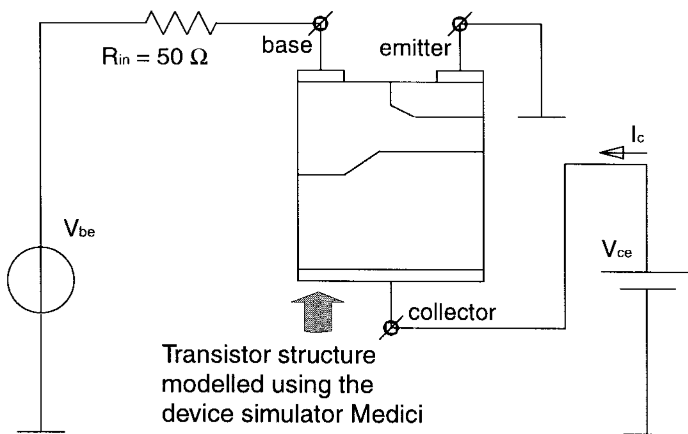

Fig. 12. Configuration used for the distortion calculation with the program MEDICI.

MAIDS fits well with the modified version of Mextram, with the previous version of Mextram exhibiting divergent behavior with increasing $V_{\rm be}$. The additional charge ΔQ_c can, depending on the value of $V_{\rm DC}(= 0.64$ V), to some extent dominate the base-collector diffusion charge $(Q_{b{\rm ctot}})$ at the onset of QS Deeper in saturation, $Q_{\rm bc}$ will become dominant over ΔQ_c. This is illustrated in Fig. 6 where ΔQ_c and $Q_{\rm bc}$ are plotted as function of the dc bias. We conclude, based on the results of Figs. 5 and 6, that with respect to the base-collector charge the modified Mextram model (with ΔQ_c) is a better representation of the physical device than the previous version of Mextram (without ΔQ_c).Alternatively, a comparable fit for the base-collector charge can be found by using the previous version of Mextram with some manipulation of the epilayer parameters (e.g. enlarging $V_{\rm DC}$). This does, however, have serious consequences for other device characteristics. By way of illustration, the 2–D device simulator MEDICI is now used to generate realistic device data. In the following discussion, one parameter set will be used which is optimized for the modified Mextram model. Figs. 7–13 all refer to the same 2-D transistor structure with the following epilayer parameters.

$R_{\rm CV}$	$1.20.10^4$ Ω
$S_{\rm CRCV}$	$4.17.10^4$ Ω
$I_{\rm HC}$	$3.93.10^{-5}$ A
$V_{\rm DC}$	0.64 V
SFH	0.53.

Part of the base-collector charge, ΔQ_c is also present in the total majority base charge (Q_b) which controls the main current I_n. This leads, when comparing the new with the previous version of Mextram, to some reduction of the collector current (ΔI_c) in the QS region for the same parameter set (see Fig. 7). Using the improved model, monotonic behavior of the Early voltages is now ensured, as is apparent when comparing Fig. 8 with Fig. 9.

At high frequencies, the addition of ΔQ_c prevents a drop in the collector charge time $(c_y/g_{{\rm epi}y})$ leading consequently to monotonic $f_T(I_c)$ behavior (see Figs. 10 and 11). This results in improved modeling of distortion as is illustrated in Fig. 13. In this figure the second-order distortion component in the collector current is shown for a 10 mV, 1 GHz input signal with the collector-base voltage maintained at 1 V. The circuit topology used for this simulation is given in Fig. 12. The nonmonotonic $f_T(I_c)$ behavior of the previous Mextram version (Fig. 10) can also be remedied by choosing $V_{\rm DC} = 0.69$ V. In Fig. 14 it may be seen that fitting the $f_T(I_c)$ characteristic by increasing the built-in base-collector voltage $V_{\rm DC}$ leads to incorrect modeling of distortion in the QS region.

VI. Conclusions

Without requiring any additional parameter the charge function ΔQ_c can be calculated based on the functional description of the base-collector depletion capacitance (c_y) and the epi-

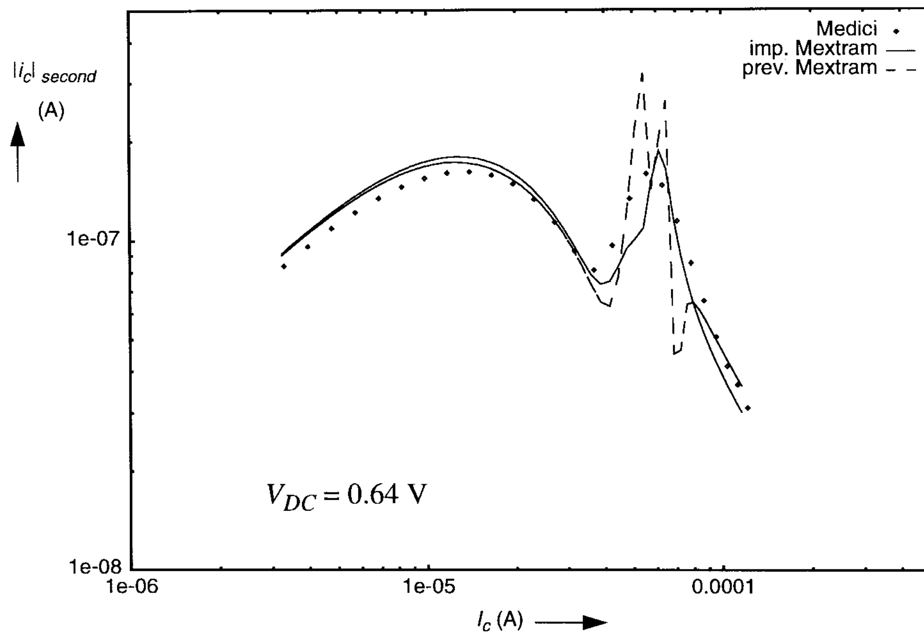

Fig. 13. The magnitude of the second-order component of the collector current.

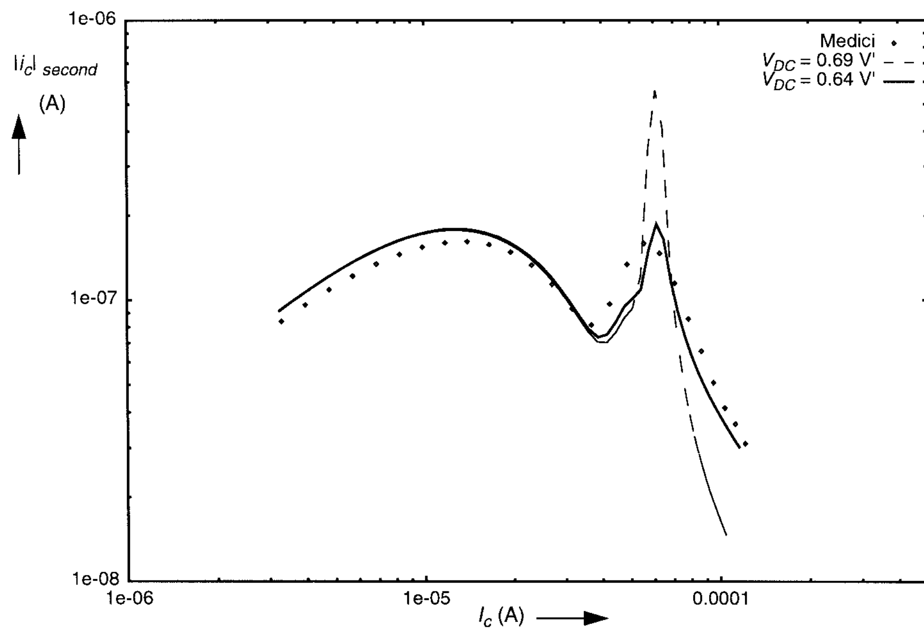

Fig. 14. The magnitude of the second-order component of the collector current compared to MEDICI using the improved Mextram model for two different values of $V_{\rm DC}$ (0.64 V and 0.69 V).

layer current $(I_{\rm epi})$. Using this formulation, ΔQ_c is not restricted to a specific epilayer model and can be calculated based on one of the epilayer models of [1], [3], [4], [7]. Incorporation of ΔQ_c in a compact bipolar model leads to greater flexibility in the modeling of the high current region of the transistor with lightly-doped epilayer. This combined with monotonic behavior at the onset of quasi-saturation yields, even for low values of $V_{\rm DC}$, a significant improvement in the modeling of the Early voltages, the $f_T(I_c)$ fall-off and the HF distortion behavior.

Modification of the Mextram model by adding this extra charge component has led to improved modeling of the distortion behavior at high frequencies when the transistor operation extends into the quasi-saturation region. Implementation of Mextram in Hewlett Packard's simulator package MDS has resulted in a very powerful combination, which facilitates the use of harmonic balance techniques in strongly nonlinear bipolar circuit design.

Appendix
The Physical Meaning of c_y and c_z

In nonquasi-saturation the small-signal value of the collector charge as a function of v_{b2c2} and $i_{{\rm epi}ns}$ [see (9) and (11)]

becomes

$$q_C = c_T \cdot v_{b2c2} + \tau \cdot i_{\text{epi}ns} = (c_T + \tau \cdot g_{\text{epi}ns})v_{b2c2} - (\tau \cdot g_{\text{epi}ns} \cdot v_{b2c1}). \quad (18)$$

With $i_{\text{epi}ns}$ given by

$$i_{\text{epi}ns} = (v_{b2c2} - v_{b2c1})g_{\text{epi}ns} \quad (19)$$

it is easily shown that

$$c_y = c_T + \tau \cdot g_{\text{epi}ns} \quad \text{and} \quad c_z = -\tau \cdot g_{\text{epi}ns}. \quad (20)$$

Here, c_T $(= c_y + c_z)$ represents the collector depletion capacitance and $\tau (= dQ_c/dI_{\text{epi}}$ at constant $V_{b2c2})$ is the delay of the mobile charge in the depletion region.

ACKNOWLEDGMENT

The authors wish to thank W. Kloosterman and M. Versleijen of Philips Research and Philips Semiconductors, respectively, for their support of the project, and W. Krans and W. Eisinga of DIMES for the use and support of the device simulation program MEDICI.

REFERENCES

[1] G. M. Kull, L. W. Nagel, S. W. Lee, P. Lloyd, E. J. Prendergast, and H. Dirks, "An unified circuit model for bipolar transistors including quasi-saturation effects," *IEEE Trans. Electron Devices*, vol. ED-32, pp 1103–1113, June 1985.

[2] H. Klose and A. W. Wieder, "The transient iIntegral charge control relation—A novel formulation of the currents in a bipolar transistor," *IEEE Trans. Electron Devices*, vol. ED-32, pp. 1090–1099, May 1987.

[3] H. Jeong and J. G. Fossum, "Physical modeling of high-current transistors for bipolar transistor circuit simulation," *IEEE Trans. Electron Devices*, vol. ED-34, p. 898, 1987.

[4] ——, "A charge-based large-signal bipolar transistor model for device and circuit simulation," *IEEE Trans. Electron Devices*, vol. 36, pp. 124–131, Jan. 1989.

[5] H. C. de Graaff and F. M. Klaasen, *Compact Transistor Modeling for Circuit Design*. New York: Springer-Verlag, 1990.

[6] MEDICI, *Two-Dimensional Device Simulation Program*, ver. 1.1, Technology Modeling Associates Inc., Mar. 1993.

[7] H. C. de Graaff and W. J. Kloosterman, *The Mextram Bipolar Transistor Model*, 1993. (implementation guide available on request from Philips Research Laboratories P.O. Box 80000, 5600 JA Eindhoven, The Netherlands.)

[8] M. P. J. G. Versleijen and A. Bauvin, "Accuracy of bipolar compact models under RF power operating conditions," in *IEEE MTT-S Tech. Dig.*, 1994, pp. 1583–1586.

[9] L. C. N. de Vreede, H. C. de Graaff, K. Mouthaan, M. de Kok, J. L. Tauritz, and R. G. F. Baets, "Advanced modeling of distortion effects in bipolar transistors using the Mextram Model," in *Proc. BCTM*, Minneapolis, MN, 1994, pp. 48–51.

[10] H. C. de Graaff and W. J. Kloosterman, "Modeling of the collector epilayer of a bipolar transistor in the Mextram model," *IEEE Trans. Electron Devices*, vol. 42, pp. 274–282, Feb. 1995.

[11] L. C. N de Vreede, H. C. de Graaff, J. L. Tauritz, and R. G. F. Baets, "Advanced modeling of distortion effects in bipolar transistors using the Mextram model," *IEEE J. Solid-State Circuits*, vol. 31. pp. 114–121, Jan. 1996.

[12] L. C. N. De Vreede, W. V. Noort, H. C. De Graaff, J. L. Tauritz, and J. Slotboom, "MAIDS: a microwave active integral device simulator," in *ESSDERC 97*, Stuttgart, Germany, Sept. 1997, pp. 180–183.

Leo C. N. de Vreede was born in Delft, The Netherlands, in 1965. He received the B.S. degree in electrical engineering from the Hague Polytechnic, Hague, The Netherlands, in 1988, and the Ph.D. degree from the Delft University of Technology, Delft, in 1996.

In the summer of 1988, he joined the Microwave Component Group of the Laboratory of Telecommunication and Remote Sensing Technology, Department of Electrical Engineering, Delft University of Technology. From 1988 to 1990, he worked on the characterization and modeling of CMC capacitors. From 1990 to 1996, he worked on modeling and design aspects of HF silicon IC's for wideband communication systems. In 1996, he was appointed Assistant Professor. He is currently working on the nonlinear distortion behavior of bipolar transistors at the Delft Institute of Microelectronics and Submicron Technology (DIMES).

Henk C. de Graaff was born in Rotterdam, The Netherlands, in 1933. He received the M.Sc. degree in electrical engineering from Delft University of Technology, Delft, The Netherlands, in 1956, and the Ph.D. degree from the Eindhoven University of Technology, Eindhoven, The Netherlands, in 1975.

He joined Philips Research Laboratories, Eindhoven, in 1964, where he worked on thin-film transistors, MOST, bipolar devices, and materials research on polycrystalline silicon. His present field of interest is device modeling for circuit simulation. Since his retirement from Philips Research in November 1991, he has been a consultant to the University of Twente and the Delft University of Technology.

Joseph L. Tauritz (S'60–M'63) was born in Brooklyn, N.Y. in 1942. He received the B.E.E. degree from New York University in 1963 and the M.S.E. degree in electrical engineering from the University of Michigan, Ann Arbor, in 1968.

He was a Research Fellow at the Delft University of Technology from 1970 to 1971. He first became acquainted with microwaves while working as a Junior Engineer on circularly polarized antennas at Wheeler Labs in the summer of 1962. From 1963 to 1970, he worked as a Technical Specialist attached to the R. F. Department of the Conduction Corporation, where he designed innovative microwave, VHF, and video circuitry for use in high-resolution radar systems. In 1970, he joined the scientific staff of the Department of Electrical Engineering, Delft University of Technology, Delft, The Netherlands, where he is presently an Associate Professor. Since 1976, he has headed the Microwave Component Group where he is principally concerned with the systematic application of computer-aided design techniques in research and education. His interests include the modeling of high-frequency components for use in the design of MIC's and MMIC's, filter synthesis, and planar superconducting microwave components.

Mr. Tauritz is a member of Eta Kappa Nu.

Roel G. F. Baets (M'88–SM'96) was born in West Belgium in 1957. He received the M.Sc. degree in electrical engineering from Stanford University, Stanford, CA, in 1981, and the B.S. and Ph.D. degrees from the University of Gent, Belgium, in 1980 and 1984, respectively.

Since 1981, he has been with the Department of Information Technology, the University of Gent. In 1989, he was appointed Professor in the engineering faculty of the University of Gent, and in 1990 he received a part-time appointment at the Delft University of Technology, Delft, The Nethelands. He has worked in the field of III–V devices for optoelectronic systems.With over 100 publications and conference papers he has made contributions to the modeling of semiconductor laser diodes, passive guided wave devices, and to the design and fabrication of OEIC's. His main interests are currently in the modeling, design, and testing of optoelectronic devices, circuits and systems for optical communication, and optical interconnects.

Dr. Baets is a member of the Optical Society of America and the Flemish Engineers Association. He has served as a member or the program committee of the ESSDERC conference of the IEEE International Laser Conference and of the ECOC conference.